

Self-gravitating systems in a three-dimensional expanding Universe

E.Aurell^{1,2,3*} and D. Fanelli^{2†}

¹ SICS, Box 1263, SE-164 29 Kista, Sweden

² Department of Numerical Analysis and Computer Science, KTH,
S-100 44 Stockholm, Sweden

³ NORDITA, Blegdamsvej 17, DK-2100 Copenhagen, Denmark

The non-linear evolution of stratified perturbations in a three-dimensional expanding Universe is considered. A general Lagrangian scheme is derived, and compared to two previously introduced, approximate, models. These models are simulated with heap-based event-driven numerical procedure, that allows for the study of large systems, averaged over many realizations of random initial conditions. One of the approximate models is shown to be quantitatively similar to the adhesion model, as concerns mass aggregation.

PACS numbers: 05.45.-a; 05.45.Pq; 04.40.-b;

I. INTRODUCTION

Structure formation in the Universe is a rich and fascinating problem, that touches many sides of Physics, from theories of the origin of primordial fluctuations, to detailed calculations of galaxy dynamics in the present epoch, including radiation pressure from stars and absorption in clouds, star birth and star mass loss. It is of great topical interest today because the recent and still improving observational data on the inhomogeneities in the cosmic microwave background radiation.

*e-mail: eaurell@sics.se

†e-mail: fanelli@nada.kth.se

Structure formation is also a challenging problem of classical Physics, i.e. how a small perturbation of a spatially almost uniform universe develops, first linearly and then non-linearly, to the pronounced structures we see today. The theory of the linear stage of this process was developed by Lifshitz [8] in the late 1940'ies, see [18,19], while the nonlinear problem can either be treated as compressible hydrodynamics, or on the kinetic level by N-body calculations or Vlasov equations. In both cases, as always in non-linear hydrodynamics and gas dynamics of large systems with many scales, approximations have to be made. These typically amount to introducing turbulent viscosities or diffusivities, either directly in modeling, or indirectly in the numerical scheme. Even so, large simulations of nonlinear gravitational instabilities are numerically difficult problems, and a good deal of expertise and familiarity with a scheme is required to evaluate the status and validity of a result.

For the reasons sketched above, there has since a long time been an interest in simplified models of structure formation. The very simplest starts from the observation that in a one-dimensional setting, gravitational attraction is a Lagrangian invariant between particle collisions. This means that starting from an initially single-stream solution, where velocity is a function of position, one can straight-forwardly compute both the linear and the non-linear behavior up the moment of caustic formation, and deduce e.g. the spectra of density perturbations up to that time. After caustic formation several approaches are possible: either one may ignore the resulting change in the gravitational force (pancake, or Zeldovich model [16]), or one may assume that its effects may be modeled by an effective diffusive term (adhesion, or Gurbatov-Saichev-Shandarin model [6]). Both these models can be solved in one, two or three dimensions, and e.g. relations between statistics of initial conditions and statistics of the solutions computed. The last model, which gives Burgers' equation, leads already to interesting probabilistic and numerical problems, surveyed in [17].

The present paper is the third in a series where we stay a little closer to the original problem than working with Burgers' equation, and study directly the collision-less self-gravitating media. One motivation is to investigate if observed self-similar behavior of the solutions of Burgers' equation also appears in a self-gravitating system. In [1] we introduced a simplified model for investigating the structure formation in an expanding Universe. This discussion will be taken up here again, in connection with the model of Rouet et al [9,12,13] for the growth of perturbations in a flat Universe. In particular, we will derive a new model that is also suitable for numerical application (*Quintic model*). In [10], in collaboration with A. Noullez, we presented an improved numerical algorithm, which takes $\mathcal{O}(\log N)$ operations per collision to simulate N particles. This new tool, extensively adopted here, allows a significant enhancement of statistics over our previous investigations.

The paper is organized as follows. In section II we derive the Newtonian approximation, starting from General Relativity. In section III we consider the special case of a stratified perturbation in a 3D homogeneous expanding Universe. Then, in section IV, we re-derive the approximate solution presented in [1]. In section V we specialize to a flat Universe and discuss the model of [9,12,13], and the new one presented here. In section VI we investigate properties of the mass distribution. Finally, in section VII we sum up and discuss our results.

II. FROM GENERAL RELATIVITY TO CLASSICAL MECHANICS

In General Relativity, points in space and time manifold are labeled by four coordinates x^μ . The Einstein conventions of covariant and contravariant indices and summation over repeated indices are assumed. The field $g_{\mu\nu}$ is (up to reparametrization) given by the solutions of Einstein's field equations

$$R_{\mu\nu} - \frac{1}{2}g_{\mu\nu}R = 8\pi GT_{\mu\nu} \quad (1)$$

where $R_{\mu\nu}$ is the curvature tensor, $R = g^{\mu\nu}R_{\mu\nu}$ its trace, $T_{\mu\nu}$ the energy-momentum tensor of the matter fields and G Newton's gravitational constant.

For a perfect fluid moving with four-velocity U relative to a given coordinate system, the energy momentum tensor is

$$T^{\mu\nu} = pg^{\mu\nu} + (p + \rho)U^\mu U^\nu \quad (2)$$

where p and ρ are the pressure and the energy density. Einsteins's equations simplify if the Universe is assumed homogeneous and isotropic, and reduce then to Freidmann's equation for a scale factor a

$$\dot{a}^2 + k = \frac{8\pi G}{3}\rho a^2 \quad (3)$$

where k is the sign of the curvature of three-dimensional slices (-1 , 0 or 1). A spatially isotropic and homogeneous metric g is given by a , e.g. in the Robertson-Walker metric with g_{tt} equal to one, $g_{rr} = -a^2/(1 - kr^2)$, $g_{\theta\theta} = -a^2r^2$ and $g_{\phi\phi} = -a^2r^2\sin^2\theta$, all off-diagonal elements zero. In a curved Friedmann Universe ($k = 1, -1$) $a(t)$ is its actual radius, but in a flat Friedmann Universe ($k = 0$) only the ratios of a 's at different times have meaning. Equation (3) should be supplemented by the law of conservation of energy $(\rho a^3)' = -3pa^2$ and an equation of state, $p = p(\rho)$.

If the energy density is dominated by non-relativistic matter, pressure can be neglected and $\rho(t) = \rho(t_0)(\frac{a(t)}{a(t_0)})^{-3}$. If the Universe is flat ($k = 0$) Friedmann's equation has the simple solution $a(t) = a(t_0)(\frac{t}{t_0})^{\frac{2}{3}}$, where the reference time t_0 , where $\rho(t_0)$ and $a(t_0)$ are given, satisfies $t_0 = (6\pi G\rho(t_0))^{-\frac{1}{2}}$. The present belief is that the Universe is actually flat or close to flat. For the slightly more complicated expressions that hold in an over-critical or an under-critical Universe, see e.g. [18].

Linear perturbations of the Einstein equations (for g), around the Friedmann solutions (where g is given by a and k), can be classified as scalar, vector and tensor, where the scalar perturbations are coupled modes of density and potential proper velocity, the vector

modes are solenoidal proper velocity fields, and the tensor perturbations are gravitational waves. If we neglect gravitational waves, Friedmann's equations and the equations for the perturbations can in fact be derived in a Newtonian setting, as explained in [18], end of section 15.1, which we will briefly recall here.

Take a spherical part S of the Universe, which is assumed homogeneous and isotropic outside S . The solutions of Einstein's equations in S do then not depend on the value of the density outside S , just as there is no gravitational force acting in Newtonian gravity on the inside of a spherical shell. For small masses Einstein gravity is well approximated by Newtonian gravity. We first assume that mass density is constant in S , equal to $\rho_b(t)$. If then S is sufficiently small and \vec{r} is a coordinate system at rest with respect to the Universe outside S , and with origin in the center of S , a particle moves according to

$$m \frac{d^2 \vec{r}}{dt^2} = -\frac{4\pi m G r^3}{3} \rho_b(t) \frac{1}{r^2} \quad (4)$$

Introducing the proper coordinate \vec{x} in S such that

$$\vec{r} = \frac{a(t)}{a(t_0)} \vec{x} \quad (5)$$

we can rewrite (4) to

$$\frac{d^2 a}{dt^2} = -\frac{4\pi G}{3} \rho_b(t) a \quad (6)$$

Equation (6) is the time-time component of the Einstein field equations (1), assuming non-relativistic matter, and also the time derivative of (3), assuming mass conservation.

We now turn to perturbations, and to simplify the notation we will write a for $a(t)$, the scale factor at time t , and a_0 and ρ_0 for $a(t_0)$ and $\rho_b(t_0)$, the scale factor and the background density at the reference time t_0 . Let the density in S at time t fluctuate around the mean value $\rho_b(t)$. The Newtonian equations of motion for N particles follow from a Lagrangian

$$\mathcal{L} = \sum_i \frac{1}{2} m_i \dot{\vec{r}}_i^2 - m_i \phi(\vec{r}_i, t) \quad (7)$$

where $\nabla_r^2 \phi = 4\pi G \rho$. By substituting the proper coordinate \vec{x} and applying the canonical transformations [11]:

$$\mathcal{L} \rightarrow \mathcal{L} - \frac{d\Psi}{dt} \quad , \quad \Psi = \sum_i \frac{1}{2} \frac{ma\dot{a}}{a_0^2} \vec{x}_i^2, \quad (8)$$

we have

$$\mathcal{L} = \sum_i \frac{1}{2} m \frac{a^2}{a_0^2} \dot{\vec{x}}_i^2 - m\varphi(\vec{x}_i) \quad (9)$$

where $\varphi = \phi + \frac{1}{2} \frac{a\ddot{a}}{a_0^2} \vec{x}_i^2$. The field equation for the new potential φ reads:

$$\nabla_x^2 \varphi = 4\pi G \rho \frac{a^2}{a_0^2} + \frac{3a\ddot{a}}{a_0^2}, \quad (10)$$

which, recalling (6), can be written [11]:

$$\nabla_x^2 \varphi = 4\pi G \left(\frac{a}{a_0} \right)^2 (\rho(\vec{x}, t) - \rho_b(t)). \quad (11)$$

Equation (11) is the starting point of our work. The source of φ is not the density itself, but the density perturbation $(\rho - \rho_b(t))$. This is as should be: in the absence of density fluctuations each particle moves according to the uniform expansion of the Universe as a whole, but remains undisturbed in the proper coordinate \vec{x} .

The equation of motion associated to the Lagrangian (9) are

$$\frac{d}{dt} \left(\frac{a^2}{a_0^2} \dot{\vec{x}} \right) + \vec{\nabla}_x \varphi(x) = 0, \quad (12)$$

where, for simplicity, we neglect from here on the label i . The peculiar velocity of a particle is not $\dot{\vec{x}}$ but $\vec{v} = \frac{a}{a_0} \dot{\vec{x}}$. The equations of motion in Eulerian form, for the peculiar velocity \vec{v} , are therefore

$$\frac{d\vec{v}}{dt} + \frac{\dot{a}}{a} \vec{v} = -\frac{a_0}{a} \vec{\nabla}_x \varphi. \quad (13)$$

Equations (13) (or (12)), (11), and the equation of continuity define the Newtonian model of structure formation we study. Closing this section, it is appropriate to summarize in what respects the model is inexact: i) it ignores gravitational waves, which are degrees of freedom of the Einstein equations with no counter-parts in Newtonian theory; ii) it is limited to weak gravitational fields, in the sense that Newtonian mechanics holds for the peculiar velocity; iii) it does not treat correctly the expansion of a local patch with a density different from the average, since density perturbations act as sources of *Newtonian* (not *Einsteinian*) gravity. Points i) and ii) are not serious for our purposes. Point iii) is actually not as problematic as it seems, since the linear growth rates in the Newtonian model agrees with the growth rates in Lifshitz' full theory of linear perturbations to the Friedmann solutions of the Einstein equations, so would only be pertinent for the nonlinear growth of perturbations of sufficiently long wave length.

III. STRATIFIED PERTURBATIONS

We now consider the special case of a stratified perturbation: the velocity has one component only and varies with respect to this direction. Initial density also only varies in this direction. In the point particle picture, the density profile which goes into the Lagrangian (7) is

$$\rho(x, t) = \sum_{x_j} m_j \left(\frac{a}{a_0} \right)^{-3} \delta(x - x_j). \quad (14)$$

where x is the comoving coordinate, in the direction of which the density and velocity varies. The Poisson equation leads to the following expression for the gravitational potential:

$$\varphi(x, t) = 2\pi \left(\frac{a}{a_0} \right)^2 G \int dy |x - y| (\rho(y, t) - \rho_b(t)). \quad (15)$$

The integral in (15) should be taken over an interval from $-L/2$ to $L/2$, L eventually taken to infinity, or to where the perturbation vanishes [1]. Equation (12) reads

$$\frac{d^2x}{dt^2} + 2\frac{\dot{a}}{a}\frac{dx}{dt} - 4\pi G\rho_b(t)x = \left(\frac{a}{a_0}\right)^{-3} E_{grav}(x, t) \quad (16)$$

where

$$E_{grav}(x, t) = -2\pi G \sum_j m_j \text{sign}(x - x_j). \quad (17)$$

The interesting thing is now that by the equation of continuity

$$\rho_b(t) = \rho_0 \left(\frac{a(t)}{a(t_0)}\right)^{-3} \quad (18)$$

the time-dependences of $4\pi G\rho_b(t)$ and $\left(\frac{a}{a_0}\right)^{-3} E_{grav}(x, t)$ are actually the same. As pointed out by Rouet et al [12,13], all time-dependence can then be concentrated in the term $2\frac{\dot{a}}{a}\frac{dx}{dt}$ by a suitable nonlinear transformation of the time variable. The choice should be

$$dt = \left(\frac{a}{a_0}\right)^{3/2} d\tau \quad (19)$$

where τ has dimension of time. Equation (16) is then transformed to

$$\frac{d^2x}{d\tau^2} + \frac{\dot{a}\sqrt{a}}{2a_0^{3/2}} \frac{dx}{d\tau} - 4\pi G\rho_0 x = E_{grav}(x, \tau) \quad (20)$$

The interest of this formulation is that, as in classical self-gravitating systems in one dimension, E_{grav} is a Lagrangian invariant, proportional to the net mass difference to the right and to the left of a given particle at a given time. Therefore, as far the particle do not experience any crossing, the equation of motion (20) reduces to the compact form:

$$\frac{d^2x}{d\tau^2} + B(\tau)\frac{dx}{d\tau} - Cx = \text{const}, \quad (21)$$

where $B(t) = \frac{\dot{a}\sqrt{a}}{2a_0^{3/2}}$ and $C = 4\pi G\rho_0$. We have hence reduced the motion between collisions to a Ricatti equation. When that can be integrated in an efficient manner, we can therefore solve general Newtonian model with a fast event-driven scheme, as in [1,3,9,12,13]. We will consider special cases when this can be done below.

IV. APPROXIMATE SOLUTION: FL MODEL

In our previous paper [1] we introduced a model we here call Friction Less (FL) model. That model basically cuts short the preceding discussion, and starts directly from equation (12) with the assumption that we consider only phenomena on time scales much less than the age of the Universe. This means that we can take a constant, alternatively that our time scales must be smaller than a/\dot{a} . By a change of the spatial scale we can set a to one, and equation (16) takes the much simpler form

$$\frac{d^2x}{dt^2} - 4\pi G\rho_0 x = E_{grav}(x, t) \quad \text{FL model} \quad (22)$$

Between collisions, (22) has solutions that are linear combination of two exponentials with rates $\pm\sqrt{4\pi G\rho_0}$. This simple form allows the implementation of a fast and exact, up to round-off errors, integration scheme [1,3]: the evolution of the system is mapped from one crossing to the next and the times the events occur are analytically computed by solving a quadratic equation. In the present paper we use a version of the new heap-based algorithm introduced in [10].

In our numerical experiment we consider a periodic perturbation with size $2L$ with reflexion symmetry. Therefore we can simulate half of the symmetric system, confining N particles in a box with reflecting edges in $-L/2$ and $L/2$. The mass of the particles is $m = N^{-1}$. We choose as unit of length the spatial interval in which the particles are initially distributed, and, thus, the initial density ρ_0 is equal to one. A natural choice of time scale is $\omega_{J0}^{-1} = (4\pi G\rho_0)^{-1/2} = \sqrt{\frac{3}{2}}t_0$, where ω_{J0} is the Jeans frequency.

In Fig. 1 we represent the evolution of the system in the phase space, starting with spatial uniform distribution. The initial velocity is a smooth function of position (first plots in Fig. 1). As the time increases the multi-stream solution takes place. The spiral-like behavior develops and the thickness of the region where velocity is not single-valued grows quickly.

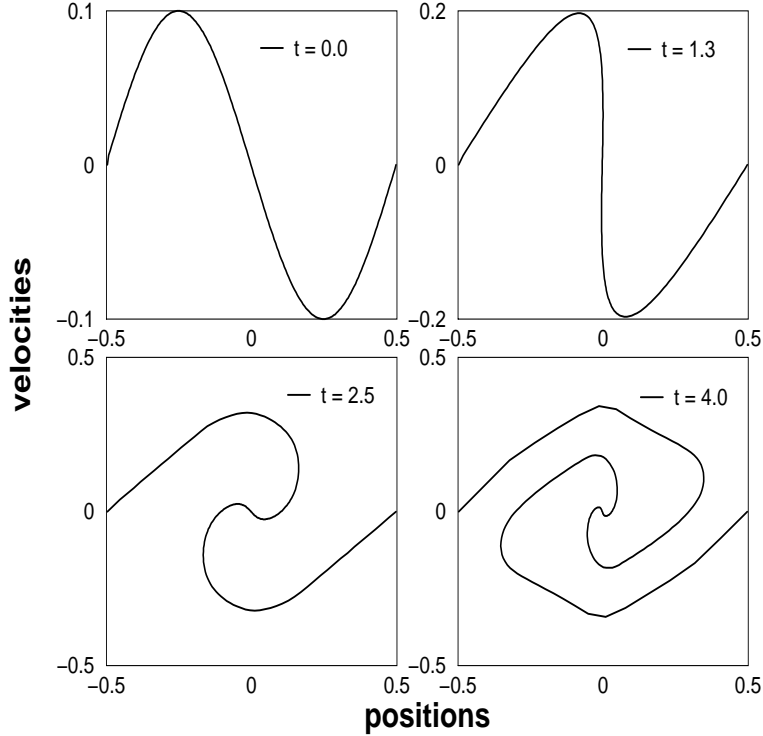


FIG. 1. Phase space portraits for the FL model with $N = 200$. The plots refer to different t , expressed in unities of Jeans' time. The first plot shows the initial velocity profile. Positions and velocities are in arbitrary units.

A. Zeldovich approximation and FL model

As a test of the validity of the FL model we establish a connection with the Zeldovich approximation, closely parallel to the similar relation for self-gravitating systems without expansion and Burgers' equation. For an extensive recent review on the subject the reader can refer to [17]. Consider the evolution of the system before the first crossing. According to eq. (22), we have:

$$\frac{d^2x}{dt^2} = \omega_{J0}^2(x - x_0), \quad (23)$$

where $x_0 = x(0)$. The solution of eq. (23) can be written in the form:

$$x = x_0 + \frac{v_0}{\omega_{J0}} \sinh(\omega_J t) \quad (24)$$

with $v_0 = v(0)$. Following a suggestion by S.N. Gurbatov, we then introduce the new time defined as $\theta = \frac{\sinh(\omega_{J0} t)}{\omega_{J0}}$ and the rescaled velocity $U = v/\dot{\theta} = v/\cosh(\omega_{J0} t)$ [7]. Thus, we get:

$$\begin{cases} x = x_0 + U(x_0)\theta \\ U(t, x_0) = U(x_0), \end{cases} \quad (25)$$

which can be combined to give the Burgers equation:

$$\frac{\partial U}{\partial \theta} + U \frac{\partial U}{\partial x} = 0. \quad (26)$$

Thus, the evolution of a particle can be thought as a free motion, by performing an appropriate rescaling of time and velocity, as far as no crossing takes place. As a less obvious consequence, the dynamics of the system can be described by macro-particles, carrying a significant part of the whole mass of the system. These macro-particles are initially located at the points of future caustic formation and evolve according to (25), as far they do not cross each other. Thus, we have access to information on the times of merging of structures without investigating the details of their inner dynamics.

As an application consider the case of the smooth initial condition represented in Fig. 2. The diamonds states for two macro-particles of mass $Nm/2$. After a time $\theta = 3.3\omega_{J0}^{-1}$ the macro-particles have collided, and, as expected, the two multi-streamed structures have merged together. Time elapsed in original coordinate is $t = 1.9\omega_{J0}^{-1}$.

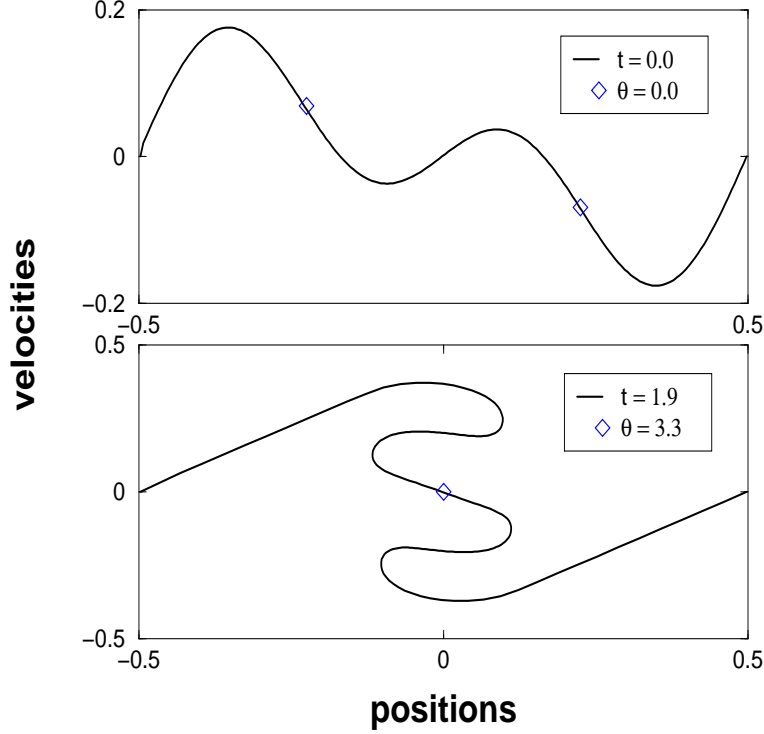


FIG. 2. The first plot shows the initial condition in the phase space. The two diamond are the macro-particles of mass $Nm/2$, initially located in correspondence of the regions where the first singularities takes place. After $\theta = 3.3\omega_{J0}^{-1}$, the macro-particles have collided, and, as predicted, the multi-stream structures merge ($t = \omega_{J0}^{-1} \sinh^{-1}(\omega_{J0}\theta) = 1.9\omega_{J0}^{-1}$). Positions and velocities are in arbitrary units.

V. MODELS OF A FLAT EXPANDING UNIVERSE

In the matter-dominated era (pressure negligible) in a flat (critical) universe ($k = 0$), the scale factor $a(t)$ grows with time as a power-law [18,19]

$$a(t) = a_0 \left(\frac{t}{t_0} \right)^{2/3}. \quad (27)$$

Here $t_0 = (6\pi G\rho_0)^{-1/2}$, as follows from equation (6). Therefore, as also pointed out by Rouet et al [12,13], the sole remaining time-dependent term in (20) becomes time-independent. Let us note that the substitution (19) can be integrated to

$$\tau = t_0 \log \frac{t}{t_0} \quad t = t_0 \exp \left(\frac{\tau}{t_0} \right) \quad (28)$$

if we make the natural non-restrictive choice that $\tau(t_0) = 0$. Equation (20) then takes the form:

$$\frac{d^2x}{d\tau^2} + \frac{1}{3t_0} \frac{dx}{d\tau} - \frac{2}{3t_0^2} x = E_{grav}(x, \tau) \quad \text{Q model.} \quad (29)$$

We refer to (29) as to the *Quintic (Q) model*. Between collisions the right-hand side of (29) is constant and the homogeneous equation has solutions

$$x(\tau) = c_1 \exp\left(\frac{2(\tau - \tau_0)}{3t_0}\right) + c_2 \exp\left(-\frac{(\tau - \tau_0)}{t_0}\right) \quad (30)$$

where c_1 and c_2 are determined by $x(\tau_0)$ and $\dot{x}(\tau_0)$ in the transformed coordinate. The form of equation (30) suggests introducing an auxiliary variable $z = \exp(\frac{\tau - \tau_0}{3t_0})$. The crossing times between consecutive particles are hence computed by solving numerically a *quintic equation* in the form:

$$b_1 z^5 - b_2 z^3 + b_3 = 0, \quad (31)$$

where the coefficients b_1, b_2, b_3 are fixed by the states of the particles at the time of the last crossing. Therefore, the event-driven scheme [10] can be adopted to follow the dynamics of this system. In comparison, however, the FL model discussed above obviously leads to a quadratic equation, and the RF model presented below, which has been the benchmark in the literature, leads to a cubic equation. Both of these can be solved algebraically, while the quintic cannot. The detail of the numerical implementation are given elsewhere [4]. In the present numerical experiments we consider a system of N particles, all of the same mass $m = N^{-1}$, confined in a finite box with reflective boundaries conditions. The unit of length is the box size and time is expressed in unit of the inverse of the Jeans frequency ω_{J0} . In Fig. 3 the evolution of the system in phase space is represented. The initial condition is the one we used for Fig. 1. As is well-known, the time evolution leads to massive central core, and the system displays the expected spiral shape. Nevertheless, due to the action of the friction term, the particles remain well concentrated in the inner zone and the thickness of the multi-stream grows much slower than in the FL.

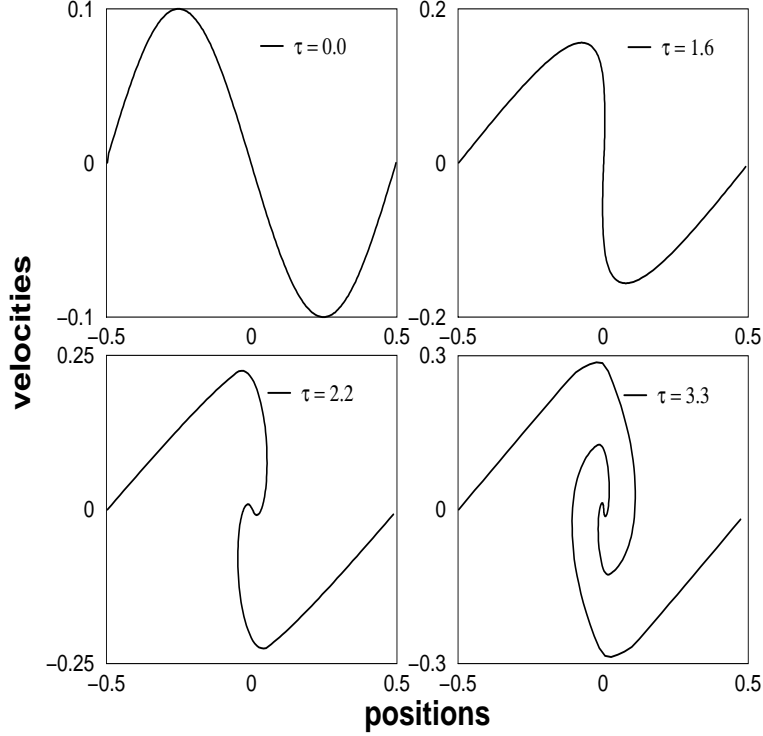


FIG. 3. Phase space portraits for Q model with $N = 200$. The plots refer to different τ , specified in the figure legends in unities of Jeans' time. In terms of cosmological time, the times elapsed after t_0 are respectively $5.79\omega_{J0}^{-1}$, $12.08\omega_{J0}^{-1}$ and $46.47\omega_{J0}^{-1}$. The first plot shows the initial velocity profile at t_0 . Positions and velocities are in arbitrary units.

Let us note the fact, that if we re-express (30) in the original time variable t using (28), and assume small initial perturbations of a uniform state, we then have, before any collisions,

$$x(t) = \tilde{c}_1 \left(\frac{t}{t_0} \right)^{2/3} + \tilde{c}_2 \left(\frac{t}{t_0} \right)^{-1}. \quad (32)$$

By the usual Eulerian-Lagrangian transformation, this means that small density perturbations develop as

$$\delta\rho(x, t) = \rho_1(x, t_0) \left(\frac{t}{t_0} \right)^{2/3} + \rho_2(x, t_0) \left(\frac{t}{t_0} \right)^{-1} \quad (33)$$

Similarly, small peculiar velocities transform according to

$$V(x, t) = v_1(x, t_0) \left(\frac{t}{t_0} \right)^{1/3} + v_2(x, t_0) \left(\frac{t}{t_0} \right)^{-4/3} \quad (34)$$

In (33) and (34) (ρ_1, v_1) is the growing mode of coupled density and velocity perturbations, while (ρ_2, v_2) is the decaying mode. It is easily checked that the growth rates in (33) and (34) agree with the ones computed directly on the Eulerian side, see [18] or [19].

A. The Rouet-Feix Model (RF)

A very interesting model was introduced about ten years ago by Rouet, Feix and collaborators [12,13], see also the recent paper [9]. One way to understand this model, in the spirit of the original derivation, is in the sense of a strictly Newtonian model of an expanding universe. Indeed, one may then specify an expansion

$$a(t) = a_0 \left(\frac{t}{t_0^{1D}} \right)^{2/3}, \quad (35)$$

without necessarily demanding, since one does not require compatibility with general relativity, that the reference time t_0^{1D} is connected to the density like in $t_0 = (6\pi G\rho(t_0))^{-1/2}$. We label the time t_0^{1D} since all change we actually have to do is to substitute (6) by the analogous 1D equation

$$\frac{d^2 a}{dt^2} = -4\pi G\rho(t)a. \quad (36)$$

From (35) and (36) follow then

$$\rho = (18\pi G t^2)^{-1} \quad t_0^{1D} = (18\pi G \rho_0)^{-1/2} = \frac{\sqrt{2}}{3} \omega_{J0}^{-1} \quad (37)$$

where $\omega_{J0} = (4\pi G \rho_0)^{1/2}$ ¹. Equation (19) can be integrated to

$$\tau = t_0^{1D} \log \frac{t}{t_0^{1D}} = \frac{1}{\sqrt{3}} t_0 \log \left(\sqrt{3} \frac{t}{t_0} \right), \quad (38)$$

¹ Note that the numerical coefficient linking t_0^{1D} to Jeans' time ω_{J0}^{-1} is equal to the inverse of the numerical constant α introduced by the authors in the derivation in [13].

which is linearly related to the τ given by (28). Between collisions equation (20) is transformed into:

$$\frac{d^2x}{d\tau^2} + \frac{\omega_{J0}}{\sqrt{2}} \frac{dx}{d\tau} - \omega_{J0}^2 x = \text{const.} \quad \text{RF model,} \quad (39)$$

which is the equation in [12,13]. The solution of the homogeneous equation takes the form:

$$x(\tau) = c_1 \exp\left(\frac{(\tau - \tau_0)\omega_{J0}}{\sqrt{2}}\right) + c_2 \exp(-\sqrt{2}(\tau - \tau_0)\omega_{J0}), \quad (40)$$

which suggests the introduction of $z = \exp(\frac{(\tau - \tau_0)\omega_{J0}}{\sqrt{2}})$, in terms of which one should solve the cubic equation

$$b_1 z^3 - b_2 z^2 + b_3 = 0 \quad (41)$$

to find the particle crossings. As in the previous case, the coefficients b_1, b_2, b_3 are fixed by the states of the particles at the time of the last crossing. We now transform back to time the coordinate t , using the second equality of (38), and find

$$x(t) = \tilde{c}_1 \left(\frac{t}{t_0}\right)^{1/3} + \tilde{c}_2 \left(\frac{t}{t_0}\right)^{-2/3}. \quad (42)$$

The exponents for the growing and decaying modes are different than in the Lifshitz-Bonner theory. Hence, the Rouet-Feix model does not predict correctly linear growth of small perturbations, and can therefore not be taken seriously as a quantitative model structure formation in a pressure-less gas in an expanding universe, obeying general relativity.

Nevertheless, the RF model has the important merit of producing a final tractable expression for computing algebraically the particle crossing times, and has qualitatively all the right ingredients of the dynamics (both friction and background terms). It can therefore be simulated by a straight-forward generalization of our heap-based event-driven scheme [10]. For a more detailed discussion of the implementation, see [5].

We note now, that at least in linear theory, there is another sense one can give to

the RF model. Namely, if q is a wave-vector of a perturbation in a comoving frame ($\delta\rho \sim \rho_q \exp(ixq)$), and we assume a non-negligible pressure $p \sim \rho^\gamma$ with $\gamma = \frac{4}{3}$, then such perturbations grow as

$$\rho_q \sim t^\alpha \quad \alpha = -\frac{1}{6} \pm \left(\frac{25}{36} - \lambda^2\right)^{1/2} \quad \lambda^2 = \frac{t^2 v_s^2 q^2}{a^2} \quad (43)$$

where v_s is the sound speed, equal to $\sqrt{\frac{\gamma p}{\rho}}$. These exponents can be matched with RF if $\lambda = 2/3$. Hence, the RF model describes the linear growth of perturbations of physical wave length $\frac{3}{2}tv_s$, which is $\sqrt{3/2}$ times larger than the instantaneous Jeans length. We note furthermore that the Jeans' length, $l_J = v_s/\sqrt{4\pi G\rho}$, scales with time as $t^{2/3}$ under the assumptions above, and that therefore the wave length of a perturbation remains in constant proportion to the Jeans wave length. The RF model may hence well have some validity also beyond linear theory. Let us add that the modifications of the values of the exponents, of (42) compared to (32), are quite reasonable. As the length scale of a perturbation approaches the Jeans length from above, the difference between expanding and decaying rates diminishes, to eventually give rise to purely oscillatory behaviour below the Jeans' length.

We now turn to simulations of the RF model. We consider a system of N particles, all of the same mass $m = N^{-1}$, confined in a finite box with reflective boundaries conditions. The unit of length is the box size and time is expressed in unit of the inverse of the Jeans frequency ω_{J0} . In Fig. 4 we show the evolution of the system in the phase space, starting with the same initial condition we used for Fig. 1. The result qualitatively agrees with the plot of Fig. 3. As for the Q model, due to the presence of the friction, the system develops a multi-stream region, that is more narrow than the one displayed by the FL. Nevertheless it has to be noticed that the process of structure formation is considerably slower, for the RF, than for the Q model. Similar phase space portraits are displayed at equal rescaled τ , but within the framework of the Q model, shorter cosmological times t are required to attain such stages (see captions of Figs. 3, 4). In addition we observe that, for similar τ , the thickness of the agglomeration is smaller in Fig 4 than in Fig. 3. A simple explanation

is, indeed, provided by looking to the relative importance of the friction and background terms, respectively in Q and RF models. In the latter, in fact, the role of the friction is overestimated and, as a consequence, the process of particles sticking is more pronounced. This observation suggests that, possibly, the adhesion model would result more similar to the approximate RF model, than to the exact Q model [4].

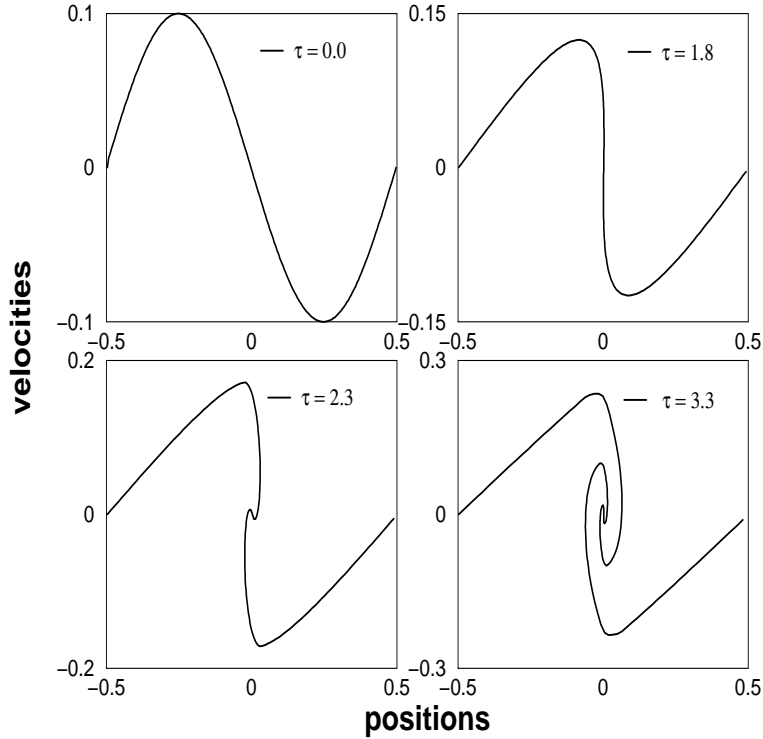


FIG. 4. Phase space portraits for RF model with $N = 200$. The plots refer to different τ , specified in the figure legends in unities of Jeans' time. In terms of cosmological time, the times elapsed after t_0 are respectively $21.4632\omega_{J0}^{-1}$, $61.9916\omega_{J0}^{-1}$ and $517.14\omega_{J0}^{-1}$. The first plot shows the initial velocity profile at t_0 . Positions and velocities are in arbitrary units.

VI. MASS OCTAVE FUNCTION

In this section we study the mass distributions for the FL, Q and RF models. Simulations are performed taking N particles initially uniformly distributed on a line of size L . Thus, the initial inter-particles distance is $\Delta x = L/N$. Velocities are generated as a Brownian

random process. This is done in the Fourier space representation where:

$$v(x) = \sum_k v_k e^{ikx} \quad (44)$$

The sum over k extends from $-\pi / \Delta x$ to $\pi / \Delta x$ in steps of $2\pi / L$ and $v_{-k} = v_k^*$. The Fourier components of positive k are then chosen as a random Gaussian independent variables with variances:

$$\langle |v_k|^2 \rangle = \frac{k^{-2h-1}}{2\Delta x}, \quad (45)$$

where h is the Hurst exponent, the scaling exponent of the second order structure functions. The choice $h = 0.5$ corresponds to standard Brownian motion. The field generated by (44) and (45) will be periodic with period L . We scale L to be one, and consider, as above, reflecting boundaries.

Fig. 5 shows a phase-space portrait for the FL model ($t = 4.0\omega_J^{-1}$). Spiral structures are displayed, as well as stretched filaments connecting the dense agglomerations. Fig. 6 represents the phase-space for the Q model at $\tau = 4.0\omega_J^{-1}$: the large-scale structures recall here even more the ones obtained in the framework of the adhesion model, even if it should be pointed out that, locally, multi-stream behaviour has in fact already started to develop (see inset in Fig. 6). Substantially similar, from a merely qualitative point of view, is the phase space portrait for the RF model, at $\tau = 4.0\omega_J^{-1}$ (see Fig. 7).

To investigate quantitatively the particle distribution, we introduce the mass octave function (MOF), already discussed in [1]. MOF measures the probability to find a non-zero contribution to the mass density, as function of the mass itself, coarse-grained in octaves. In other words, $P(\Delta m)$ is the cumulative probability of finding Δm in an octave interval $[m_k, m_{k+1}[$, where $m_k = 2^{-k}$ ($k = 0, 1, \dots$). Practically, the MOF analysis reveals the degree of dishomogeneity of a probability distribution, since in terms of the MOF a uniform distribution would correspond to a logarithmic histogram with only one non-zero entry. The

main plot of Fig. 8 show, in doubly logarithmic scale, the MOF computed for RF at an intermediate stage of evolution ($\tau = 3.3\omega_{j0}^{-1}$). In a finite range the mass octave function displays a power-law decay with exponent -0.5 . This result is in agreement with [2,14] where, in the framework of the adhesion model, the number density per unit length of shock locations holding mass m is shown to be distributed as power-law m^{-1-h} .

Figs. 9 show the MOF for a later time evolution of the RF model. An approximate power law regime is found (see small inset), and a numerical fit gives exponent $\alpha^{RF} = -0.25$.

The main plot of Fig. 10 represents the MOF for the Q model at rescaled time $\tau = 3.0\omega_{j0}^{-1}$. There is no evidence of a transient power-law state, with slope -0.5 , as shown for the RF. This observation again indicates that the adhesion picture is, in fact, closer to the RF model, than to the exact Q approach. The small inset displays, in doubly logarithmic scale, the MOF for the Q model at $\tau = 3.0\omega_{j0}^{-1}$ and $\tau = 5.5\omega_{j0}^{-1}$. In the latter case an approximate power-law, over a finite mass support, is displayed and the best numerical fit gives exponent $\alpha^Q = 0.1$.

Figs. 11 shows on the other hand the MOF for the FL model. At an intermediate stage, ($\tau = 4.0\omega_{j0}^{-1}$) the MOF is clearly not uniform, but best described as a structure with two peaks. At later times an approximate power-law regime is found, with a positive exponent ($\alpha^{FL} = 0.4$, at $\tau = 5.5\omega_{j0}^{-1}$).

We observe that the exponent α^Q is practically equidistant from the values of α^{RF} and α^{FL} . Nevertheless α^Q is positive, and therefore, concerning the mass aggregation, the exact Q dynamics is shown to be qualitatively more similar to the FL model, than to the RF. This is, indeed, a very surprising conclusion.

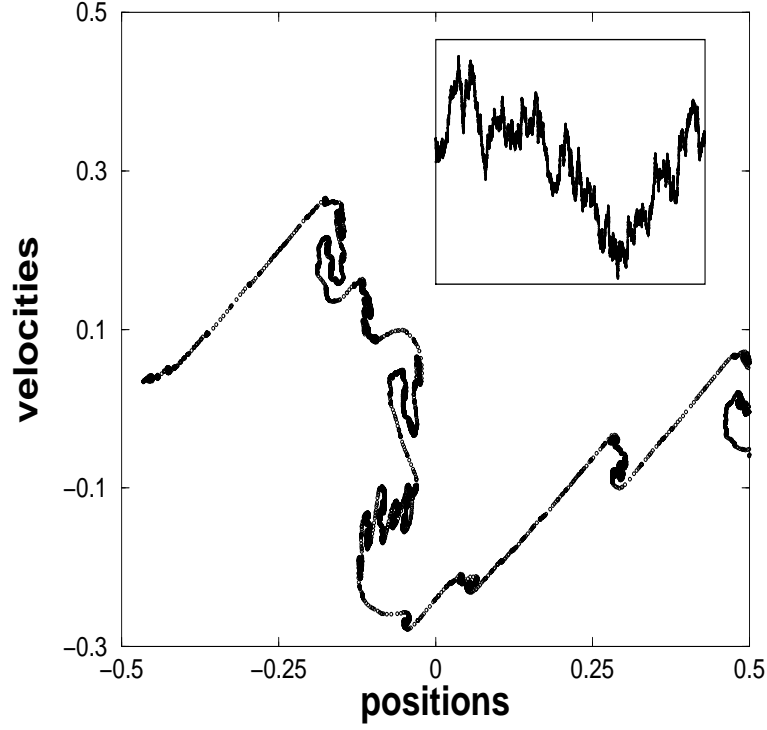


FIG. 5. Velocity field vs. position, for FL model, starting from a single-speed Brownian motion initial conditions (small inset). Here $N = 16384$ and $t = 4.0\omega_{J0}^{-1}$. Reflecting boundaries are assumed. Positions and velocities are in arbitrary units.

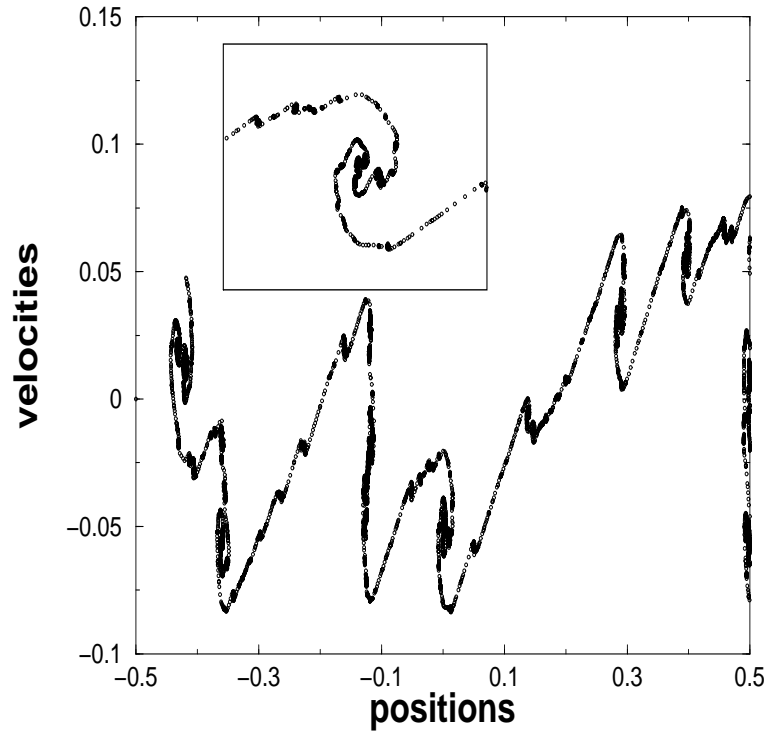


FIG. 6. Velocity field vs. position, for Q model, starting from a single-speed Brownian motion initial conditions. Here $N = 16384$ and $\tau = 4.0\omega_{J0}^{-1}$ (or $t = 109.53\omega_{J0}^{-1}$). Reflecting boundaries are assumed. The inset is a zoom of a massive agglomeration. Positions and velocities are in arbitrary units.

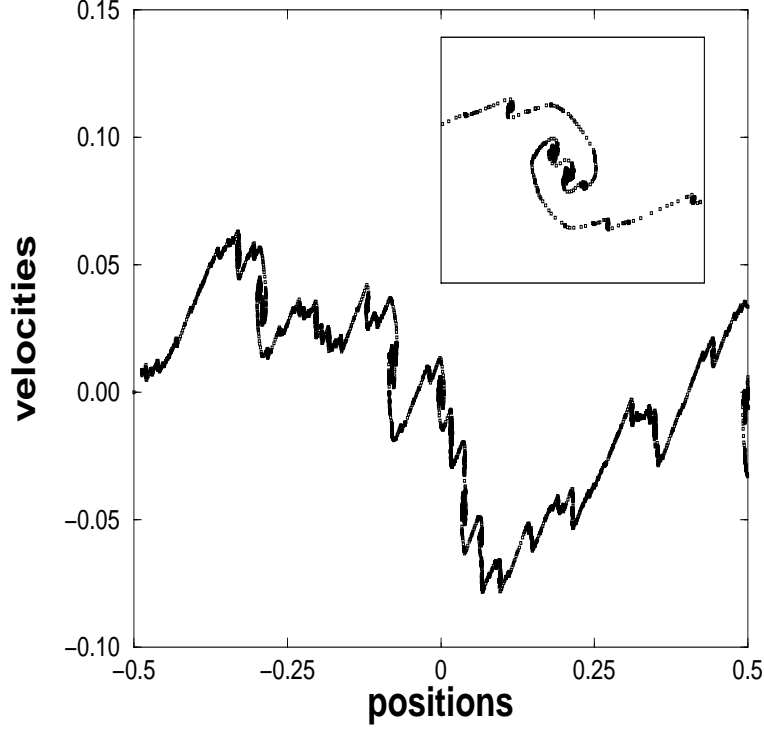


FIG. 7. Velocity field vs. position, for RF model, starting from a single-speed Brownian motion initial conditions. Here $N = 16384$ and $\tau = 4.0\omega_{J0}^{-1}$ (or $t = 2.283 \times 10^3\omega_{J0}^{-1}$). Reflecting boundaries are assumed. The inset is a zoom of a massive agglomeration. Positions and velocities are in arbitrary units.

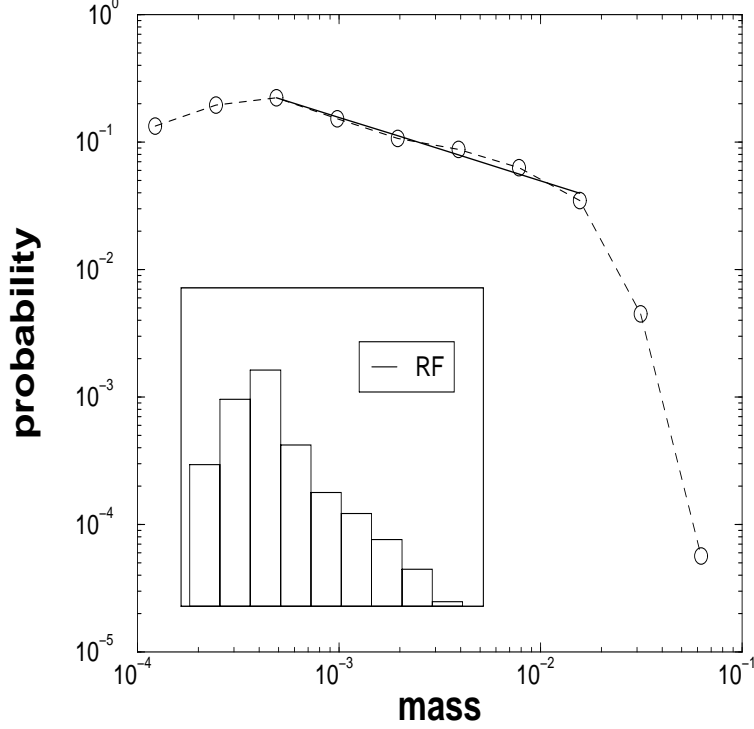


FIG. 8. Log-log normalized mass distribution in octaves (MOF) for Brownian initial velocities for RF (dashed line) at time $\tau = 3.3\omega_{j_0}^{-1}$ (or $t = 517.14\omega_{j_0}^{-1}$). The number of particles is 16384, number of independent realizations 1000. The height of a column is the fraction of a total number of bins containing mass in the range $[m, 2m]$. The bin size is $l = 0.00195$, a uniform density would hence correspond to a single column at abscissa 0.00195 and ordinate 1.0. An intermediate power-law regime is clearly displayed for RF model. The best numerical fit gives exponent $\alpha = -0.5$ (solid line). The small inset represents the MOFs in log-lin scale. Mass is in arbitrary units.

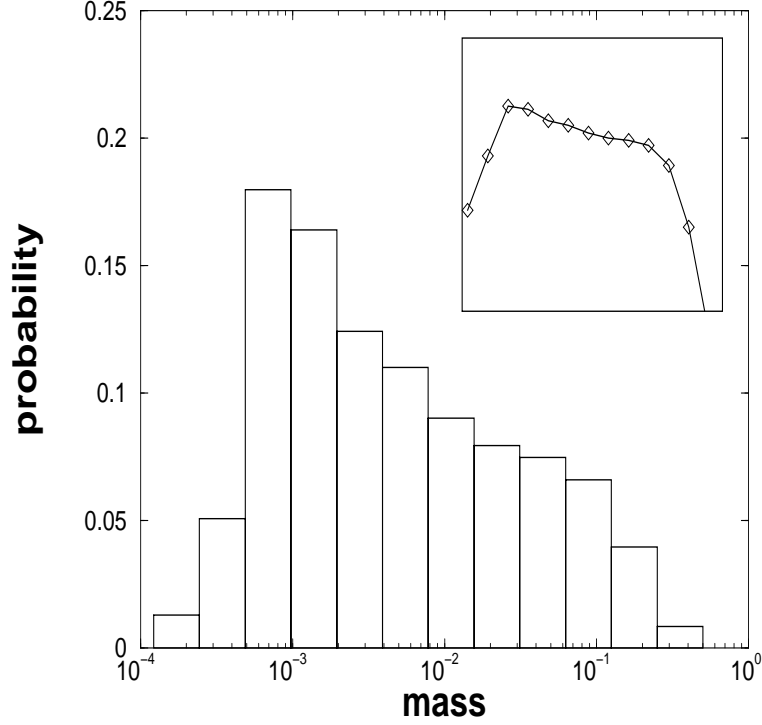


FIG. 9. Normalized mass distribution in octaves (MOF) for Brownian initial velocities at $\tau = 5.5\omega_{J_0}^{-1}$ (or $t = 5.5007 \times 10^4 \omega_{J_0}^{-1}$), for RF model. The number of particles is 8192, number of independent realizations 1000. The bin size is $l = 0.01562$. The small inset is a plot of the MOF in log-log scale. A numerical fit to a power law gives exponent $\alpha^{RF} = -0.25$. Mass is in arbitrary units.

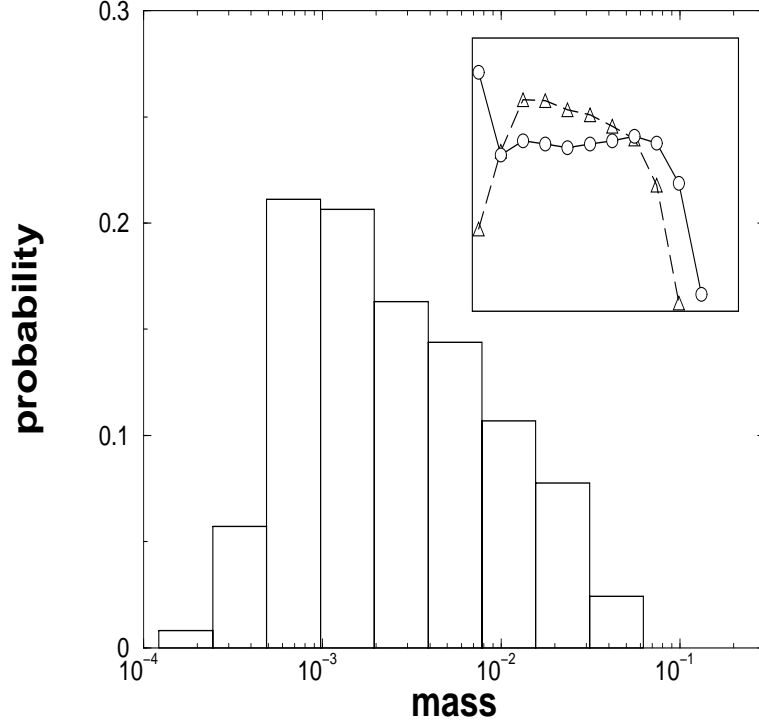


FIG. 10. Normalized mass distribution in octaves (MOF) for Brownian initial velocities at $\tau = 3.0\omega_{J0}^{-1}$ (or $t = 32.18\omega_{J0}^{-1}$), for Q model. The number of particles is 8192, number of independent realizations 500. The bin size is $l = 0.003906$. The small inset represents the MOF in log-log scale for respectively $t = 3.0\omega_{J0}^{-1}$ (dashed line and triangles) and $\tau = 5.5\omega_{J0}^{-1}$ ($t = 687.71\omega_{J0}^{-1}$, solid line and circles). Bin size, number of particles and number of independent realizations as for the main figure. An intermediate power-law regime, with positive exponent, develops as the evolution is pushed forward. The best numerical fit gives exponent $\alpha^Q = 0.1$ at $\tau = 5.5\omega_{J0}^{-1}$. Mass is in arbitrary units.

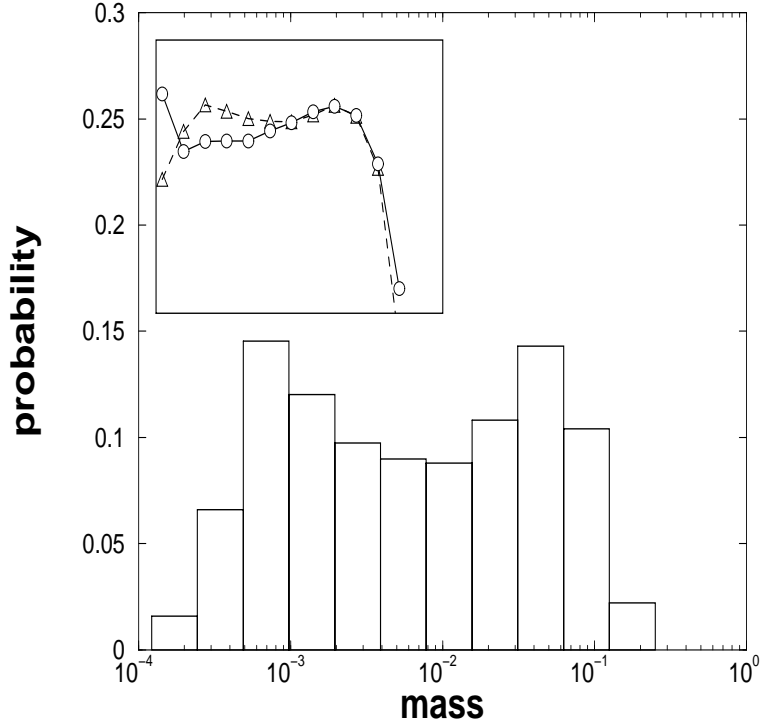


FIG. 11. Normalized mass distribution in octaves (MOF) for Brownian initial velocities at $t = 4.0\omega_{J0}^{-1}$, for FL model. Number of particles and number of realizations as in Fig. 9. The bin size is $l = 0.01562$. The small inset represents the MOF in log-log scale for respectively $t = 4.0\omega_{J0}^{-1}$ (dashed line and triangles) and $t = 5.5\omega_{J0}^{-1}$ (solid line and circles). Bin size, number of particles and number of independent realizations as for the main figure. An intermediate power-law regime develops as the evolution is pushed forward. The best numerical fit gives exponent $\alpha^{FL} = 0.4$ at $t = 5.5\omega_{J0}^{-1}$. Mass is in arbitrary units.

VII. CONCLUSIONS

In this paper we have discussed the problem of structure formation in a three-dimensional expanding Universe, focusing on stratified perturbations in a collision-less medium. We derived a representation of the Lagrangian development of such perturbations from the linear regime to large times, which forms the basis of an efficient numerical scheme (Q model). In practice, this scheme requires solving automatically a large number of quintic equations, the coefficients of which are only known at run-time, and therefore entails algorithmic problems

that are discussed in [4].

We then re-derived as approximate solutions the Friction Less Model (FL), recently introduced in [1], and the Rouet-Feix (RF) model, and compared them to the exact Q dynamics. Quantitatively, the growth of small perturbations differs between RF and Q; the RF model is in this sense more similar to growth of finite wave length perturbations in a model with non-zero pressure. Numerical simulations have been carried out for smooth and random initial perturbations, and phase space portraits, respectively for FL, RF and Q, have been computed. The latters show compact collapsed structures, visually more like the shock waves (singular mass agglomerations) in the adhesion model (Burgers' equation).

To make our analysis more quantitative, we studied the statistics of mass distributions from random initial conditions. For intermediate times, when the multi-stream behaviour is not well developed, the RF model agrees well with the scaling law for the frequency of agglomerations of given size containing mass m in Burgers equation [15,14,17], i.e. $s(m) \sim m^{-1-h}$. This is not true for either the Q or the FL model. In particular, the FL seems to tend to a bifractal structure, with either very high or very low density agglomerations.

We finally studied the late time behaviour of the FL, Q and RF models. All then display states which seem to have approximate power-law MOF. The actual states are however different, with the most numerous mass agglomerations in FL (positive α^{FL}) having about equal mass (they then also carry most of the mass), while the most numerous mass agglomerations in the RF (negative α^{RF}) are still small, and carry a small proportion of the mass. The exponent α^Q , characteristic of the Q dynamics, is practically equidistant from α^{RF} and α^{FL} . Nevertheless α^Q is positive and, therefore, surprisingly enough, we are led to conclude that, concerning the mass aggregation, the exact Q dynamics is qualitatively more similar to the FL model than to the RF model.

Summing up, we have compared three models for studying the evolution of a stratified perturbation in an expanding universe. Only the Q model is in quantitative agreement with the linear theory of growth of perturbations to the Friedmann solutions of the Einstein equations. Quantitatively, the approximate RF is shown to agree with the adhesion model, with respect to the mass aggregation.

ACKNOWLEDGMENTS

We thank S.N. Gurbatov, B. Miller, P. Muratore-Ginanneschi, A. Noullez and J.L. Rouet for discussions. This work was supported by the Swedish Research Council through grants NFR I 510-930 (E.A.) and NFR F 650-19981250 (D.F).

-
- [1] Aurell E., Fanelli D. & Muratore-Ginanneschi P., “On the dynamics of a self-gravitating medium with random and non-random initial conditions”, *Physica D* **148** 272 (2001).
 - [2] Aurell E., Frisch U., Noullez A. & Blank M. “Bifractality of the Devil’s staircase appearing in the Burgers equation with Brownian initial velocity”, *J Stat Phys.* **88**, 1151 (1997)
 - [3] Eldridge O.C. & Feix M., “One-dimensional plasma model at Thermodynamic equilibrium”, *The Physics of Fluids* **5** (1962), 1076-1080.
 - [4] Fanelli D. & Aurell E. “Asymptotic behaviour of a stratified perturbation in a three dimensional expanding Universe”, preprint.
 - [5] Fanelli D., Aurell E. & Noullez A., to be published in the Proceeding of IAU Symposium 208, *Astrophysical Supercomputing using Particle Simulations*.
 - [6] Gurbatov S.N., Saichev A.I. & S.F. Shandarin S.F., “The large-scale structure of the Universe in the frame of the model equation of non-linear diffusion”, *Monthly Notices of the Royal Astronomical Society* **236** (1989) , 385-402.

- [7] Gurbatov S.N. (2000), [private communication].
- [8] Lifshitz E., *J. Phys. USSR* **10** (1947), 116.
- [9] Miller B. & Rouet J.-L., “Influence of expansion on hierarchical structures for the study of one-dimensional particle systems”, astro-ph/0106117
- [10] Noullez A., Fanelli D. & Aurell E., “A heap-based algorithm for the study of one-dimensional particle systems”, submitted to Journ Comp. Phys., cond-mat/0101336
- [11] Peebles P.J., *The Large-scale Structure of the Universe*, Princeton,NJ: Princeton University Press, 1980.
- [12] Rouet J.L., M.R. Feix & Navet M., “One-dimensional numerical simulation and homogeneity of the expanding universe”, *Vistas in Astronomy* **33** (1990), 357-370.
- [13] Rouet J.L. et al, “Fractal properties in the simulation of a one-dimensional spherically expanding universe”, in *Lecture Notes in Physics: Applying Fractals in Astronomy* (1991), 161-179.
- [14] She S.-Z., Aurell E. & Frisch U., “The inviscid Burgers equation with initial data of Brownian type” *Comm. Math. Phys.* **148** (1992), 623-641.
- [15] Sinai Ya.G. “Statistics of shocks in solutions of inviscid Burgers equation” *Comm. Math. Phys.* **148** (1992), 601-622.
- [16] Shandarin S.F. & Zeldovich Ya.B., “The large scale structure of the Universe: turbulence, intermittency, structures in a self gravitating medium”, *Rev. Mod. Phys.* **61** (1989), 185-220.
- [17] Vergassola M., Dubrulle B., Frisch U. & Noullez A., “Burgers’ equation, Devil’s staircases and the mass distribution for large-scale structures”, *Astron. & Astrophys.* **289** (1993) 325-356.
- [18] Weinberg S., *Gravitation and Cosmology*, Wiley (1972).
- [19] Zeldovich Ya.B. & Novikov I.D., *Stroenie i evoljucija vselennoj* [The Structure and the evolution of the Universe], Nauka Moscow (1974).